ISBN: 978-3-95450-225-7 ISSN: 2673-5571 doi:10.18429/JACoW-HB2021-THDC2

COMMISSIONING OF THE ESS FRONT END

N. Milas*, R. Miyamoto, C. S. Derrez, E. M. Donegani, M. Eshraqi, B. Gålnander, H. Hassanzadegan, E. Laface, Y. Levinsen, M. Muñoz, E. Nilsson, C. Plostinar, A. G. Sosa, R. Tarkeshian and C. Thomas
European Spallation Source ERIC, Lund, Sweden

Abstract

The European Spallation Source, currently under construction in Lund, Sweden, will be the brightest spallation neutron source in the world, when the proton linac driver achieves the design power of 5 MW at 2 GeV beam energy. Such a high power requires production, efficient acceleration, and transport of a high current proton beam with minimal loss. This implies in a challenging design and beam commissioning of this machine. The linac features a long pulse length of 2.86 ms at a relatively low repetition late of 14 Hz. The ESS ion source and low energy beam transport are in-kind contributions from INFN-LNS. Beam commissioning of this section started in September 2018 and continued until early July in 2019. This article presents highlights from a campaign of beam characterizations and optimizations during this beam commissioning stage.

ION SOURCE AND LEBT OVERVIEW

European Spallation Source (ESS), currently under construction in Lund, Sweden, will be a spallation neutron source driven by a proton linac [1]. The beam commissioning of the ESS linac is being be conducted in stages [2–4]. Commissioning of the first and stage, consisting of the Ion Source (IS) and LEBT, started in September 2018 and continued until early July in 2019. The IS of ESS is a microwave discharge type with the nominal extraction voltage of 75 kV. This type of source is known to produce a high current and high quality beam. As indicated in Table 1, the beam out of the IS includes other ion species, typically around 20% and primarily H_2^+ and H_3^+, which are lost still within the LEBT section. After stable operation was established, the IS provided more than 400 hours of beam time by the end of the beam commissioning period.

Figure 1 is a schematic layout of the LEBT, showing the locations of the two solenoids and other devices. Each solenoid has an integrated pair of dipole correctors (*steerers*) acting on both transverse planes. In between the solenoids, inside the *Permanent Tank,* there are one Faraday Cup (FC), a set o Beam Induced Fluorescence Monitors (BIFMs) [5], and Emittance Measurement Units (EMUs) of Allison scanner type measuring for vertical plane. Beam Current Monitors (BCMs) measure the IS extraction current and also the LEBT output current. The LEBT also houses an iris, which is a movable diaphragm with six blades that mechanically restricts the aperture to adjust the beam current, and a chopper, which adjusts pulse length by deflecting the leading and

* natalia.milas@esss.se

Table 1: ESS IS Possible Operational Parameters

Parameter	Value	Unit
Energy	~75	keV
Peak current (total)	~85	mA
Peak current (proton)	~70	mA
Proton fraction	~80	%
Pulse length	~6	ms
Pulse repetition rate	14	Hz
Duty cycle	~8	%

trailing parts of a pulse. During this first stage of beam commissioning a temporary tank, referred to as *Commissioning Tank*, was placed right after the collimator at the end of the LEBT, providing additional measurement locations closer to the RFQ interface. Inside this *Commissioning Tank* a second EMU (measurement the vertical plane as well) was installed and a second pair of BIFs was available. The use of the BIFMs in a LEBT is a relatively new idea and provided a tool to perform conventional diagnostics techniques, such as an emittance reconstruction based on a gradient scan, even for this part of the linac. Examples of characterizations based on the BIFMs will be presented when discussing the Linear Optics studies in the LEBT.

SOURCE TUNING

In order to tune the IS a scan of 5 parameters is required: the 3 coils confining the magnetic field inside the plasma chamber (referred as Coil 1, 2, and 3, counting from the extraction side), the input RF power for the magnetron and the injected H_2 flux. It was found the source output current was specially sensitive to the Coil 2 strength. Figure 2 shows

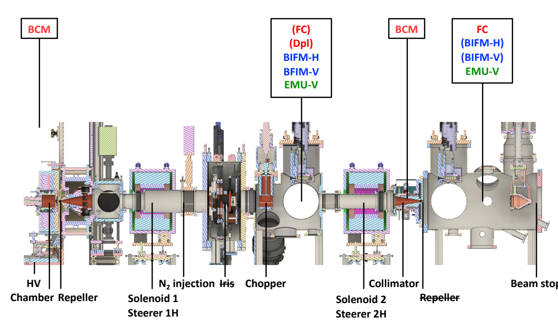

Figure 1: Schematics of the ESS IS and LEBT. a) Close-up of the IS plasma chamber and extraction system. b) IS and LEBT with diagnostics devices.

64th Adv. Beam Dyn. Workshop High-Intensity High-Brightness Hadron Beams HB2021, Batavia, IL, USA JACoW Publishing
ISBN: 978-3-95450-225-7 ISSN: 2673-5571 doi:10.18429/JACoW-HB2021-THDC2

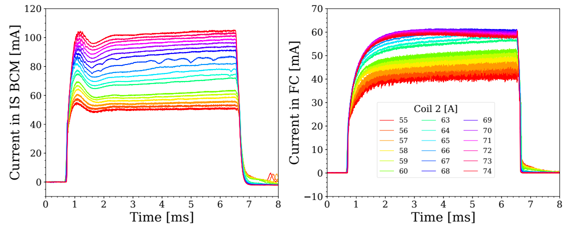

Figure 2: Beam pulses during a Coil 2 scan. a) Measurement with the IS BCM. b) Measurement with the FC in the Permanent Tank. (RF power, Coil 1 current, Coil 3 current, and H_2 flux were kept to 500 W, 120 A, 217 A, and 3.5 sccm.)

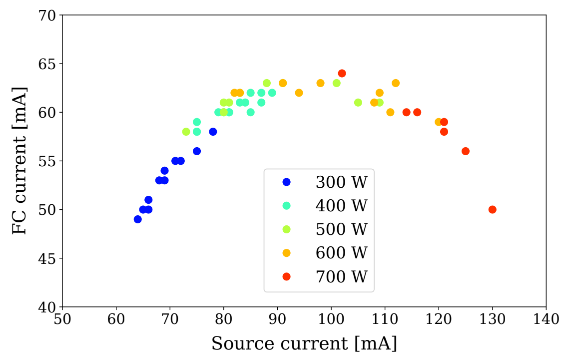

Figure 3: Relations between currents out the IS and those measured in Permanent Tank with the FC for various IS settings. (Strengths of Solenoid 1, Steerer 1H, and Steerer 1V were kept to 249 mT, −2.72 mT, and −0.35 mT.)

changes in beam pulse shapes during a scan of Coil 2 current, observed by the IS BCM (2a) and FC in Permanent Tank (2b). We defined the Coil 2 current of 67-68 A as the optimal setting, for the fixed values of the other four parameters. It was also found that a small increase in the H_2 flux tends to compensate the drooping effect. Thus, the H_2 flux was used to fine-tune the flatness after an optimal Coil 2 current was found.

During the study, the magnetron power and currents in Coil 1 and Coil 3 were scanned and a local optimal setting for each combination was found. Figure 3 summarizes the result of the study, showing the relations between the total currents (averaged over the 2.9 ms plateau) extracted from the IS and those measured by the FC in Permanent Tank. During the study, Solenoid 1 was kept to a fixed value to make an almost parallel (slightly converging) beam and likewise the first set of steerers were adjusted to maximize the current measured by the FC. As seen in the figure, the current out of the IS is correlated with the magnetron power, as expected, but also depends a lot on strengths of the coils. Another important feature is that the current reaching the Permanent Tank is highly correlated with the current out of the IS. This indicates that the condition of the meniscus and the initial divergence are also highly correlated with the extracted current.

Figure 4 shows the measured beam pulses and vertical phase space distributions for two settings, a Standard Setting where the standard current expected for this source in nominal operations is extracted and a Low Setting with a extracted current of 60 mA from the source. The Low Setting has a slower rise time, and the extracted pulse length has to be extended to achieve the same level of flatness as the Standard Setting. Each setting has different values for the magnetron power and coils that were adjust in order to extract the best possible beam. The discrepancy between the LEBT BCM and FC has not been well understood [6], and further investigation has to be conducted. The phase space distribution of the Standard Setting not only has a larger emittance but also features the wing-like structure, often due to an imperfect meniscus condition or a solenoid aberration. The LEBT of ESS has an injection point of N_2 gas right after the IS extraction system which can be used to spoil the vacuum level intentionally and increase the degree of space charge neutralization. The emittance measurements of Figures 4c and 4d were repeated for various levels of N_2 flux as well (0.1 to 9 sccm), but no positive effect was observed, indicating a large initial divergence at the IS which also causes a large beam size filling the aperture of Solenoid 1. This large initial beam divergence is still under study and more experiments are planned for the following commissioning round in 2021 in order to understand it.

BEAM TRANSPORT IN THE LEBT

Trajectory and Linear Optics

The LEBT section is required to transport the proton beam to the RFQ with minimal losses and provide the required Courant-Snyder parameters at the interface. In addition, the beam has to enter the RFQ with minimal position and angular offsets, since the transmission and output beam quality of the RFQ are sensitive against these offsets. A set of BIFMs at two different locations allow measurements and corrections

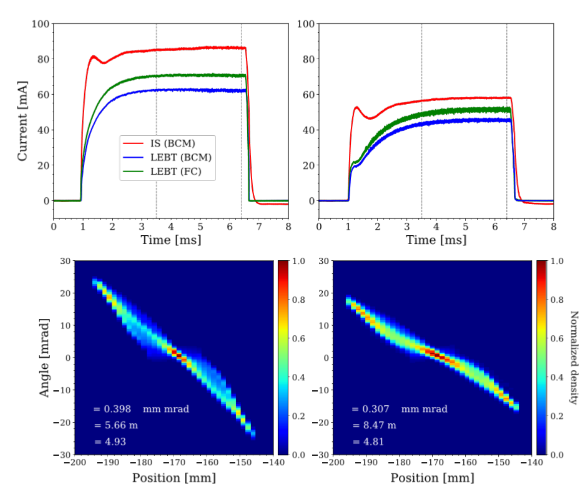

Figure 4: Measured beam pulses and phase distributions for Standard and Low Settings. a) Pulses for Standard Setting. b) Pulses for Low Setting. c) Vertical phase space distributions in Permanent Tank for Standard Setting. d) Vertical phase space distributions (vertical plane) in Permanent Tank for Low Setting.

ISBN: 978-3-95450-225-7 ISSN: 2673-5571 doi:10.18429/JACoW-HB2021-THDC2

of trajectory in the ESS LEBT. The conventional scheme of simply minimizing the offset at each monitor location was possible, but another method of characterizing the beam near the image point condition was adopted to identify error sources [7].

When the centroid position is measured near the image point of a lens (Solenoid 1) and its strength is scanned, information of error sources can be acquired as fit parameters to a model. Thus, the key to the method is to determine the Solenoid 1 strength to produce the image point at the BIFMs. Note that in the considered example, the main error sources are tilts of Solenoid 1 and the initial trajectory errors out of the IS. Solenoids offsets were estimated to be negligible compared to those errors, as long as they are within the specified alignment tolerances of 100-200 µm [7]. Figure 5a shows a scan of the beam size as a function of Solenoid 1 strength. As seen in the figure, identifying the condition for the image point is fairly trivial. Figure 5b shows a more detailed scan around the image point; in this particular case, the strengths of Solenoid 1 to minimize the beam sizes at the BIFMs were 282.7 mT for the horizontal plane and 283.7 mT for the vertical plane. Once the condition for the image point is identified, the rest of method is relatively straightforward model fitting against the scan around the image point condition [7]. The curves of the beam sizes for Solenoid 1 strengths too weak or too strong flatten out. This indicates that the beam is being clipped at some element before the BIFMs, implying that the measurements are untrustworthy for both beam size and centroid position in those regions.

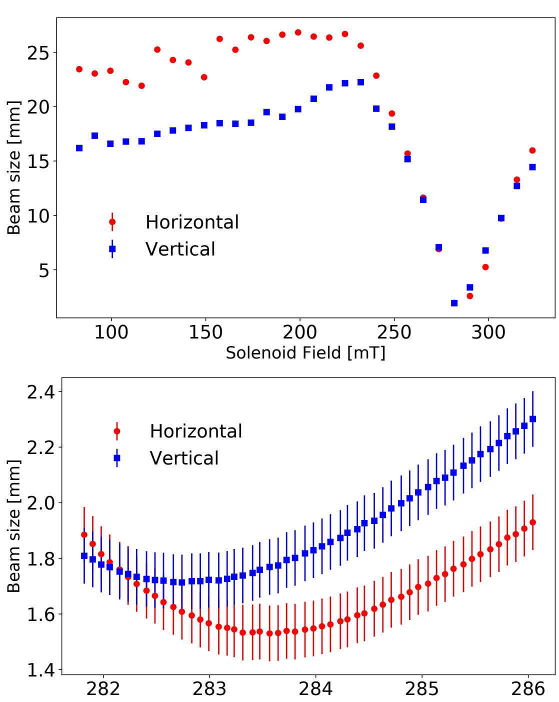

Figure 5: a) Beam size measured with the BIFMs in Permanent Tank as a function of Solenoid 1. b) Close-up around the image point.

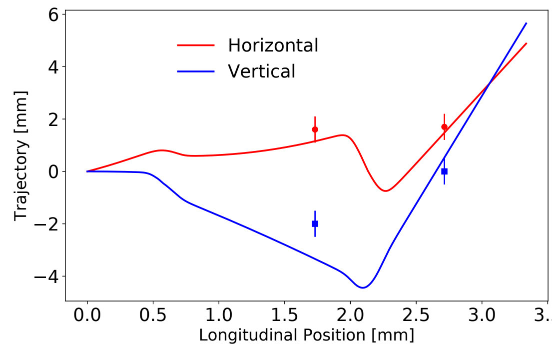

Figure 6: Comparison between the modeled trajectory (lines) and measured positions at BIFMs (markers) in the LEBT.

This situation ultimately affects accuracy of the corrected trajectory by always requiring high Solenoid 1 strengths for the measurements, which are not ideal for evaluating the initial angles at the IS.

Based on the method described above, a series of measurements were performed during the beam commissioning period to assess the initial angular error at the IS and solenoid tilts, and the mean values obtained for both solenoids tilts and source misalignment are listed in Table 2. Note, for the reconstruction of the solenoid tilts, the mean value of measurements from both planes are listed. A large tilt in each solenoid was predicted from the field measurement prior to their delivery and the presented method qualitatively confirmed this, but discrepancies are remaining in terms of magnitude. In order to verify the reconstructed solenoid tilts and initial angular errors at the IS, the beam trajectory was simulated through the LEBT with the reconstructed errors, for a set of solenoid strengths weaker than those corresponding to the image point condition (259.5 mT for Solenoid 1 and 211.4 mT for Solenoid 2), and the simulated centroid positions at both sets of BIFMs were compared with the measurements. As seen in Figure 6, the model predictions and measurements are in fairly good agreement.

Solenoids Scan

The standard technique to match the beam to the RFQ is to scan the solenoids and find the strengths that maximize transmission. For a typical RFQ, such a condition almost coincides with that for the best emittance preservation, and this is also the case for the RFQ of ESS [8–11]. As seen in [12], the pattern of the LEBT output current during the solenoids scan could also provide indirect information of var-

Table 2: Measurements Results for Solenoid and Source Errors

Elements	θ **[mrad].**	ϕ **[mrad]**	xp_0 **[mrad]**	yp_0 **[mrad]**
Source	-	-	1.3±0.3	0.0±0.4
Solenoid 1	−1.0±0.5	−4.0±0.1	-	-
Solenoid 2	2.0±0.7	7.0±2.0	-	-

ISBN: 978-3-95450-225-7 ISSN: 2673-5571 doi:10.18429/JACoW-HB2021-THDC2

ious conditions of the IS and LEBT. Hence, the effects from the reconstructed solenoid tilts and initial angular errors, as well as (empirically acquired) larger initial RMS sizes and angles, were tested in simulations of the solenoids scan. The simulations were performed with TraceWin code [13] by assuming a space charge compensation level of 95%. Figure 7 shows the measured currents with the BCM at the RFQ interface for different sets of solenoid strengths (a) and their simulations (b, c and d). Comparison of Figure 7b and Figure 7c demonstrates the difference of taking into account those reconstructed errors. Better agreement with the measurement (a) is visible for the case with the errors (c), especially for the reduction in current in the region between the weak-focusing and strong-focusing regions. On the other hand, the region with a high transmission is still much larger for the simulation, and further improvements are expected if a more realistic initial distribution at the IS can be achieved. Measurements of emittance and Courant-Snyder parameters in the Permanent Tank indicated that the initial beam out the IS has an RMS angle larger than the simulated [14] and Figure 7d shows the simulation emulating such a larger initial RMS angle case, together with the reconstructed errors. Further improvement in agreement with the measurement (a) indicates the right direction in terms of correcting the initial distribution for simulations.

Matching to RFQ

For both IS settings, Standard and Low Settings discussed before, we performed EMU measurements in the Commissioning Tank for different sets of solenoid strengths. This was to understand a trend of the matching condition to the RFQ. As representative cases, three sets of measurements are shown in Figure 8. The reconstructed emittance and mis-

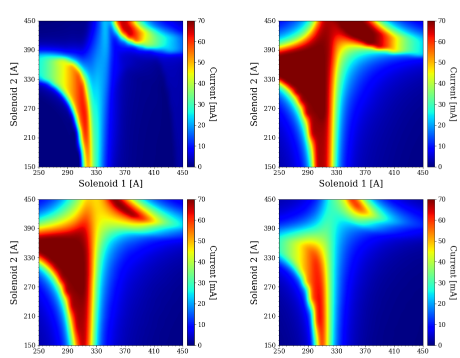

Figure 7: LEBT output current against scan of two solenoids. a) Measurements from the BCM at the RFQ interface. b) Simulation using the nominal simulated initial distribution with an emittance of 0.144 π mm mrad, $\beta = 0.44$ m and $\alpha = -4.23$ and with no error. c) Simulation using the nominal initial distribution and with the reconstructed solenoid tilts and initial angular errors. d) Simulation using the initial distribution with increased initial $\beta = 0.7$ m and $\alpha = -10.0$ and with the reconstructed solenoid tilts and initial angular errors.

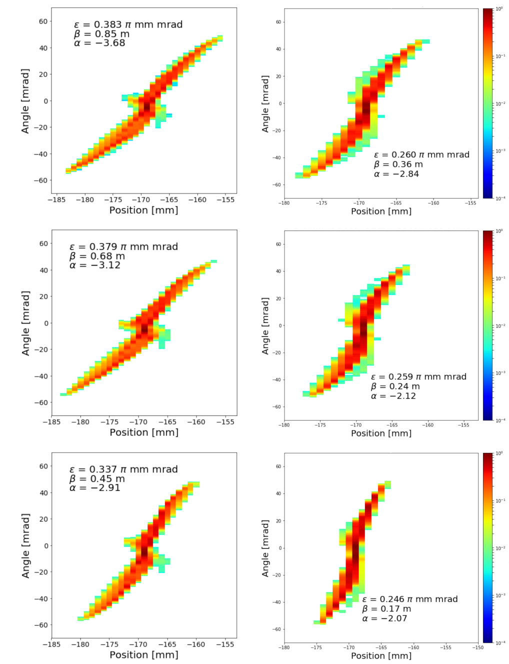

Figure 8: EMU measurements in Commissioning Tank with different solenoid strengths, for two IS setting. For the IS setting, left column: Standard Setting and right column: Low setting. For the solenoid strengths, top row: (258, 216) mT, middle row: (258, 207) mT and bottom row: (254, 216) mT.

match parameter [15] at the RFQ interface (with respect to $\beta = 0.17$ and $\alpha = 1.7$ from the most recent simulation [8]) are summarized in Table 3. Compared to the measurements in the Permanent Tank (Figure 4), there is a ~5% reduction in emittance for the Standard Setting and ~15% for the Low Setting. The reduction seen for the third set of the solenoid strengths is due to a small loss of current. The mismatch parameter at the RFQ interface, which is 149.5 mm upstream of the EMU, was estimated approximately by simple propagation of the Courant-Snyder parameters in a drift ignoring space charge. As seen in the table, the tested sets of solenoid strengths were not far from the well matched condition for the Low Setting, whereas this was not the case for Standard Setting. Preparing a good matching condition from direct measurement at the EMU in the Commissioning Tank is not at all trivial, since it depends strongly on beam current,

Table 3: Emittance and Estimated Mismatch at the RFQ Interface for Tested Sets of Solenoid Strengths

IS setting	**Solenoids [mT]**	**Emittance [π mm mrad]**	**Mismatch [%]**
Standard	(258, 216)	0.38	211
	(258, 207)	0.38	172
	(254, 216)	0.34	91
Low	(258, 216)	0.26	55
	(258, 207)	0.26	22
	(254, 216)	0.25	21

emittance, and even details in the distribution used initially. In addition, an accurate reconstruction of the beam parameters at the RFQ interface requires knowledge of the level of space charge compensation which is not available and for this reason the matching will rely strongly on optimization of the transmission through the RFQ.

LESSONS LEARNED

At the very beginning of the commissioning we experienced grounding issues both at the IS and LEBT which delayed commissioning by approximately 5 months. The corrections required several months of consolidation works against high-frequency discharges, but afterwards achieved reliable and stable operation. Due to the lack of proper grounding some equipment were damaged, including power supplies that had a long fixing/replacing lead time. Since we started commissioning with no spare parts readily available for any of the systems, this resulted in several weeks of recommissioning, once the main grounding issue was resolved, with just partial systems active. Another issue that was present throughout commissioning was a constant struggle with the integration of many systems. As a consequence some of the equipment that was intended to be tested during the LEBT commissioning never became fully functional (as the Iris) or had very poor performance and will have to be retested or recommissioned, e.g. the cases for the LEBT Chopper and the repeller at the end of the LEBT. Since there was no time allocated for integrated tests before commissioning these obstacles should not have come as a surprise. For the next commissioning round we planed ahead to have integrated tests and dry runs before beam extraction in order to save commissioning time for beam tests only.

From the Beam Physics point of view, we were not able to explain the larger emittance (>0.4 π mm mrad for 70 mA protons out of LEBT) and larger initial divergence then the ones observed during the off-site commissioning [16, 17]. This large emittance is not reproducible with the extraction code and more investigation on this topic is of high importance for us to fully understand the IS. Another issue we observed was a large trajectory deviation, which resulted in the need to have larger kicks on the dipole correctors in order to maximize current transmission through the LEBT cone and which cannot be easily explained either. Given all this open issues, a test stand for source study and characterization is being assembled at ESS.

CONCLUSION

This article presented selected highlights from the first beam commissioning activities at ESS for its IS and LEBT. The IS initially experienced grounding issues and required several months of consolidation works against high-frequency discharges, but afterwards achieved reliable and stable operation. It demonstrated great flexibility in tuning and production of the required level of current, but on the other hand the observed emittance was larger than the design value of 0.25 π mm mrad near the RFQ interface, unless the current was lowered significantly. The cause and mitigation of the emittance larger than expected, as well as impact to the downstream sections when such a beam is injected to the RFQ, will continue to be investigated as a part of preparations for the upcoming beam commissioning stages, covering the normal-conducting injector. In addition to the conventional Allison scanner type EMU, BIFMs were used for characterizations of the beam trajectory and profiles in the LEBT and proved to be extremely useful. During the IS and LEBT commissioning we faced a series of issues, from grounding to integration. Going forward, we included integrated test ahead of beam extraction in the schedule in order to minimize issues appearing during beam commissioning.

REFERENCES

[1] R. Garoby *et al.*, "The European Spallation Source Design", *Phys. Scr.*, vol. 93, p. 014001, 2018. doi:10.1088/1402-4896/aa9bff

[2] R. Miyamoto, M. Eshraqi, and M. Muños, "ESS Linac Plans for Commissioning and Initial Operations", in *Proc. HB'16*, Malmö, Sweden, July 2016, pp. 342-347. doi:10.18429/JACoW-HB2016-TUPM5Y01

[3] R. Miyamoto, M. Eshraqi, M. Muños, and C. Plostinar, "Beam Commissioning Planning Updates for the ESS Linac," in *Proc. IPAC'17*, Copenhagen, Denmark, May 2017, pp. 2407-2410. doi:10.18429/JACoW-IPAC2017-TUPVA131

[4] C. Plostinar *et al.*, "Opportunities and Challenges in Planning the Installation, Testing and Commissioning of Large Accelerator Facilities", in *Proc. 9th Int. Particle Accelerator Conf. (IPAC'18)*, Vancouver, Canada, Apr.-May 2018, pp. 878–881. doi:10.18429/JACoW-IPAC2018-TUPAF065

[5] C. A. Thomas *et al.*, "Commissioning of the Non-invasive Profile Monitors for the ESS LEBT", in *Proc. 8th Int. Beam Instrumentation Conf. (IBIC'19)*, Malmö, Sweden, Sep. 2019, pp. 495–498. doi:10.18429/JACoW-IBIC2019-WECO04

[6] C. S. Derrez *et al.*, "Initial Performance of the Beam Instrumentation for the ESS IS & LEBT", in *Proc. 10th Int. Particle Accelerator Conf. (IPAC'19)*, Melbourne, Australia, May 2019, pp. 2650–2653. doi:10.18429/JACoW-IPAC2019-WEPGW076

[7] N. Milas *et al.*, "Beam Based Alignment of Elements and Source at the ESS Low Energy Beam Transport Line", in *Proc. 8th Int. Beam Instrumentation Conf. (IBIC'19)*, Malmö, Sweden, Sep. 2019, pp. 600–604. doi:10.18429/JACoW-IBIC2019-WEPP032

[8] E. Nilsson, M. Eshraqi, J. F. Esteban Müller, Y. Levinsen, N. Milas, and R. Miyamoto, "Beam Dynamics Simulation with an Updated Model for the ESS Ion Source and Low Energy Beam Transport", in *Proc. 10th Int. Particle Accelerator Conf. (IPAC'19)*, Melbourne, Australia, May 2019, pp. 1042–1045. doi:10.18429/JACoW-IPAC2019-MOPTS083

[9] R. Miyamoto *et al.*, "Preparation towards the ESS Linac Ion Source and LEBT Beam Commissioning on ESS Site", in *Proc. 9th Int. Particle Accelerator Conf. (IPAC'18)*, Vancouver, Canada, Apr.-May 2018, pp. 874–877. doi:10.18429/JACoW-IPAC2018-TUPAF064

ISBN: 978-3-95450-225-7 ISSN: 2673-5571 doi:10.18429/JACoW-HB2021-THDC2

[10] Y. Levinsen *et al.*, "European Spallation Source Lattice Design Status", in *Proc. 6th Int. Particle Accelerator Conf. (IPAC'15)*, Richmond, VA, USA, May 2015, pp. 3911–3914.

[11] Y. Levinsen, L. Celona, M. Eshraqi, and L. Neri, "In-depth Analysis and Optimization of the European Spallation Source Front End Lattice", in *Proc. 7th Int. Particle Accelerator Conf. (IPAC'16)*, Busan, Korea, May 2016, pp. 1274–1277. doi:10.18429/JACoW-IPAC2016-TUPMR020

[12] Ø. Midttun, L. Celona, B. Cheymol, R. Miyamoto, L. Neri, and C. Thomas, "Measurements and Simulations of the Beam Extraction from the ESS Proton Source", in *Proc. 17th Int. Conf. on Ion Source*, Geneva, Switzerland, Oct. 2017, p. 080022. doi:10.1063/1.5053377

[13] D. Uriot and N. Pichoff, "Status of TraceWin Code", in *Proc. 6th Int. Particle Accelerator Conf. (IPAC'15)*, Richmond, VA, USA, May 2015, pp. 92–94. doi:10.18429/JACoW-IPAC2015-MOPWA008

[14] Ø. Midttun, "Off-site commissioning report for the ESS proton source and LEBT", ESS Rep. ESS-0190279, 2018.

[15] K. R. Crandall and D. P. Rusthoi, "TRACE 3-D documentation, third edition", Los Alamos Rep. LA-UR-90-4146, 1997.

[16] L. Neri *et al.*, "Beam Commissioning of the High Intensity Proton Source Developed at INFN-LNS for the European Spallation Source", in *Proc. 8th Int. Particle Accelerator Conf. (IPAC'17)*, Copenhagen, Denmark, May 2017, pp. 2530–2532. doi:10.18429/JACoW-IPAC2017-WEOBB2

[17] L. Celona *et al.*, "Ion Source and Low Energy Beam Transport Line Final Commissioning Step and Transfer from INFN to ESS", in *Proc. 9th Int. Particle Accelerator Conf. (IPAC'18)*, Vancouver, Canada, Apr.-May 2018, pp. 1712–1714. doi:10.18429/JACoW-IPAC2018-TUPML073